FACULTY OF INFORMATION TECHNOLOGY AND ELECTRICAL ENGINEERING

DEGREE PROGRAMME IN WIRELESS COMMUNICATIONS ENGINEERING

BACHELOR'S THESIS

mmWave ANTENNA DESIGN IN 5G MOBILE PHONES

Author Wei Zhang

Supervisor Kimmo Rasilainen

February 2026

Wei Z. (2026) **mmWave Antennas Design in 5G mobile phones.** University of Oulu, Faculty of Information Technology and Electrical Engineering, Degree Programme in Electronics and Communications Engineering. Bachelor's Thesis 28 p.

ABSTRACT

5G wireless technology operates across a wide range of frequency bands, classified into Frequency Range 1 (FR1) and Frequency Range 2 (FR2). FR1 includes frequencies below 7.225 GHz, many of which are also utilised in existing 4G systems. In contrast, FR2 encompasses millimetre-wave (mmWave) bands, which enable data transfer rates of up to 10 Gbit/s—nearly 100 times faster than 4G. However, integrating multiple antennas within the limited space of modern 5G mobile devices presents a significant challenge for antenna designers.

This thesis addresses these challenges by first examining the key differences between sub-6 GHz and mmWave antennas in mobile phones, with a particular focus on the design trade-offs involving antenna size, efficiency, and bandwidth. The study also explores state-of-the-art mmWave antenna design solutions, drawing from both academic research and industry advancements. Furthermore, this thesis discusses and compares various proposed solutions while also reviewing Specific Absorption Rate (SAR) standards and regulatory limits for both sub-6 GHz and mmWave frequencies, ensuring compliance with global safety regulations.

By providing a comprehensive analysis of 5G antenna design challenges and potential solutions, this thesis aims to contribute to the development of efficient and practical mmWave antennas for next-generation mobile devices.

Key words: mmWave, 5G, mobile antennas.

TABLE OF CONTENTS

FOREWORD

This bachelor's thesis explores the challenges and solutions associated with mmWave antenna design for 5G mobile phones. Throughout this journey, I have received invaluable support and guidance from several individuals, to whom I am deeply grateful.

I extend my sincere gratitude to my thesis supervisor, Dr. Kimmo Rasilainen, for his expert guidance, insightful feedback, and unwavering support throughout my research. I am also grateful to Timo Kurjenheimo, antenna specialist at Aava Mobile Oy, for his assistance with CST simulations and technical expertise, which significantly contributed to my work.

Finally, I would like to express my heartfelt appreciation to my family—my wife, Yi Zhang, and my son, Kaiwen Zhang—for their unwavering support, patience, and encouragement throughout my studies and thesis work. Their belief in me has been a constant source of motivation.

Oulu, February 1st, 2026

Wei Zhang

LIST OF ABBREVIATIONS AND SYMBOLS

3GPP	3rd generation partnership project
4G	Fourth Generation
5G	Fifth Generation
AoC	Antenna on Chip
AoP	Antenna on Package
AoD	Antenna on Display
AiD	Antenna in Display
AR	Augmented Reality
BLER	Block error rate
CDF	Cumulative Distribution Function
CST	Computer Simulation Technology
DRL	Dosimetric reference limit
eMBB	Enhanced Mobile Broadband
EIRP	Equivalent isotropic radiated power
EMF	Electromagnetic Fields
FCC	Federal Communications Commission
FWA	Fixed Wireless Access
FR1	Frequency Range 1, between 410 MHz and 7,125 MHz
FR2	Frequency Range 2, between 24,250 MHz and 71,000 MHz
G_r	Receiver Antenna Gain
G_t	Transmitter Antenna Gain
IEEE	Institute of Electrical and Electronics Engineers
ICNIRP	International Commission on Non-Ionizing Radiation Protection
IoT	Internet of Things
ICNIRP	International Commission on Non-Ionizing Radiation Protection
L_{FS}	Free Space loss
LTE	Long Term Evolution
MIMO	Multiple Input Multiple Output
mMTC	Massive Machine Type Communications
QoS	Quality of Service
RL	Exposure reference levels
SAR	Specific Absorption Rate
TRP	Total Radiated Power
URLLC	Ultra Reliable Low Latency Communications
UE	User Equipment
VR	Virtual Reality
WiFi	Wireless fidelity
λ	Wavelength
ρ	Density
Pr	Received power
Pt	Transmitted Power

1 INTRODUCTION

Fifth-generation (5G) mobile communication systems are designed to support a wide range of data-intensive and latency-sensitive services, leading to substantial improvements in wireless connectivity. Compared with previous generations, 5G smartphones are expected to operate under more demanding scenarios, including immersive multimedia applications and emerging intelligent systems. These requirements impose stringent constraints on achievable data throughput, latency performance, and spectral utilization, thereby increasing the complexity of radio-frequency front-end and antenna system design across multiple frequency bands. In particular, maintaining high antenna efficiency within compact mobile devices while enabling multi-band operation represents a fundamental challenge for contemporary 5G antenna implementations.

This thesis focuses on antenna design challenges in 5G mobile terminals, with particular emphasis on millimeter-wave (mmWave) solutions. Key design parameters relevant to mmWave antennas are analyzed, followed by a comparative evaluation of several representative state-of-the-art 5G mobile phone antenna architectures. Furthermore, international Specific Absorption Rate (SAR) regulations and compliance requirements are reviewed over a broad frequency range extending from sub-6 GHz to mmWave bands, as user safety considerations remain an essential aspect of mobile antenna design.

The remainder of this thesis is organized as follows. Chapter 2 introduces the fundamental concepts of 5G communication systems, including typical application scenarios and key performance indicators. Chapter 3 analyzes mmWave propagation mechanisms and the primary factors influencing signal transmission. Chapter 4 presents fundamental principles of sub-6 GHz and mmWave antenna design, highlighting major design challenges and representative 5G antenna solutions. Chapter 5 provides a comparative performance analysis of different mobile phone antenna configurations. Chapter 6 reviews SAR standards and regulatory limits over frequencies ranging from 100 MHz to 300 GHz. Chapter 7 outlines a systematic design procedure for mmWave antennas in mobile devices, and Chapter 8 concludes the thesis with a summary of key findings and potential directions for future research.

2 OVERVIEW OF 5G TECHNOLOGY

Fifth-generation (5G) mobile communication systems represent the evolutionary advancement beyond 4G LTE, with design objectives cantered on improving data throughput, latency performance, and network flexibility. To meet diverse service requirements, 5G operates across a wide range of frequency bands, each offering distinct propagation characteristics and capacity trade-offs.

Lower-frequency bands are primarily employed to provide wide-area coverage due to their favourable propagation properties, although their achievable data rates are constrained by limited spectral resources. These bands are commonly utilized in applications requiring extensive geographic reach rather than peak throughput. In contrast, frequency bands above 6 GHz, typically referred to as mid-band or FR1, offer a compromise between coverage and capacity. Owing to their moderate propagation range and increased bandwidth availability, mid-band frequencies have become a preferred choice for deploying advanced technologies such as massive multiple-input multiple-output (MIMO) in dense urban environments.

At higher frequencies, millimeter-wave (mmWave) bands, also known as FR2, enable access to significantly larger bandwidths, allowing substantially higher data rates over short communication distances. While these bands can support multi-gigabit-per-second throughput, their propagation is more susceptible to attenuation and blockage, resulting in reduced coverage and smaller cell sizes. Consequently, mmWave systems rely heavily on dense network deployments and highly directional antenna arrays to compensate for increased path loss. The combination of low-, mid-, and high-frequency bands therefore enables 5G networks to balance coverage, capacity, and service quality across different deployment scenarios.

2.1 5G application areas

According to the International Telecommunication Union Radiocommunication Sector (ITU-R), 5G use cases can be broadly classified into three categories: enhanced Mobile Broadband (eMBB), massive Machine-Type Communications (mMTC), and ultra-Reliable and Low-Latency Communications (URLLC) [ITU-R]. These categories encompass a wide range of services, from high-data-rate applications to large-scale device connectivity and mission-critical communications.

Table 1. 5G use cases

mMTC	**eMBB**	**URLLC**
• Lighting and road sign control	• Immersive AR/VR	• Industrial automation
• Smart Waste Management	• Advanced gaming, 8k video streaming	• Intelligent Transportation
• Asset tracking	• Enterprise broadband connectivity	• Remote healthcare
• Structure and environmental monitoring	• Connected transportation infotainment	• Drone communications

From a system design perspective, 5G networks are intended to support a diverse set of communication requirements that differ significantly in terms of data rate, latency, reliability, and connection density. One major category focuses on enabling connectivity for a massive number of low-complexity devices, many of which transmit small amounts of data intermittently and are constrained by strict power consumption requirements. Supporting such large-scale deployments places strong demands on network scalability, coverage, and energy efficiency.

Another category emphasizes high-throughput mobile services driven by user-centric applications. These services require sustained high data rates, low interruption time, and efficient utilization of radio resources to accommodate bandwidth-intensive content and interactive multimedia experiences. As a result, network capacity and spectral efficiency become critical performance considerations.

A third category addresses communication scenarios where transmission reliability and latency are of primary importance. In such cases, the network must provide highly stable connections with extremely low end-to-end delay to support time-sensitive operations. Typical examples include automated control systems, cooperative vehicular functions, and remote operation scenarios, where communication failures or excessive latency may lead to safety or operational risks.

These three categories broadly correspond to the enhanced Mobile Broadband (eMBB), massive Machine-Type Communications (mMTC), and ultra-Reliable and Low-Latency Communications (URLLC) use cases defined by the International Telecommunication Union Radiocommunication Sector (ITU-R) [ITU-R].

2.2 5G performance

The performance of a 5G network is commonly evaluated using indicators such as transmission speed, latency, error rate, and coverage capability. Research reported by Ericsson indicates that 5G generally achieves lower latency than 4G, particularly when operating in millimeter-wave frequency bands, where the smallest delays are observed. In practical deployments, most recorded latency values for both 4G and 5G remain under 50 milliseconds [1]. Nevertheless, from an end-user perspective, overall network experience is more strongly associated with achievable data rates than with latency alone [1].

Speed: 5G technology utilizes a wide range of frequency bands, each characterized by different performance and coverage properties.

- Low-band(Sub-6 GHz, approximately 600 MHz–2.4 GHz) 5G supports broad geographic coverage but relatively limited throughput. Typical download speeds range from about 50 Mbps to 250 Mbps, which represents only a modest improvement compared to many 4G networks, where speeds often stay below 30 Mbps. These gains are largely enabled by Massive MIMO technology and other improvements beyond traditional LTE implementations.
- Mid-band(Sub-6 GHz, approximately 3–6 GHz) 5G offers a compromise between coverage area and data rate, enabling performance levels that generally vary from around 100 Mbps up to 1 Gbps.
- Millimeter-wave (mmWave, approximately 24–60 GHz) bands provide the highest potential data rates, with peak values theoretically reaching between 10 and 20 Gbps.

Latency: Latency represents one of the most notable performance differences between fourth- and fifth-generation mobile systems. 5G networks are designed to support extremely low delays, often below 5 milliseconds, whereas 4G systems typically exhibit latency in the range of approximately 60 to 98 milliseconds. This substantial reduction is especially important for applications that require near real-time responses, such as autonomous transportation systems and industrial automation.

Error Rate: Both 4G and 5G networks employ block error rate (BLER) as a standard indicator for assessing radio link reliability. Common target values are around 2% for synchronized operating conditions and approximately 10% for out-of-synchronization scenarios. Maintaining BLER within these limits supports stable and efficient wireless communication.

Coverage Range: The coverage area of a 5G base station is strongly dependent on the operating frequency band.

- Low and mid bands: Macro base stations using these frequencies typically provide coverage distances of roughly 1.6 km to 5 km.
- High band (mmWave):Small cells deployed in millimeter-wave bands usually cover much shorter distances, often between 15 and 600 meters.

Due to the propagation characteristics of millimeter-wave signals, including high attenuation and weak penetration through obstacles such as walls, buildings, and even the human body, dense deployments of small cells are required to ensure continuous connectivity, particularly in urban environments.

3 MILLIMETER WAVE PROPAGATION PROPERTIES

Millimeter-wave (mmWave) signals have wavelengths on the order of one to several millimeters. In comparison with sub-6 GHz frequencies, mmWave signals exhibit distinctly different propagation behaviour. For this reason, a clear understanding of their transmission characteristics is essential when analysing high-frequency wireless systems.

3.1 Free space pathloss

Under line-of-sight (LOS) conditions, the relationship between transmitted and received power can be described using the Friis transmission formula:

$$L_{FS} = Pr/Pt = G_t \; G_r \; (\lambda \; / \; 4\pi d)^2 \tag{1}$$

where P_r denotes the received power, P_t is the transmitted power, d represents the separation distance between transmitter and receiver, G_t and G_r are the antenna gains, and λ is the signal wavelength. For isotropic antennas, both antenna gains are equal to 1 (0 dB). By expressing the equation in terms of frequency and converting to decibels, the free-space path loss can be written as:

$$L_{FS\,dB} = 20\log(d) + 20\log(f) + 32.44 \tag{2}$$

Adding back the antenna gains, the line-of-sight pathloss becomes equation (3)

$$L_{FS\,dB} = -G_t - G_r + 20\log(d) + 20\log(f) + 32.44 \tag{3}$$

Taking 28 GHz as an example, the free-space path loss is approximately 29 dB higher than at 1 GHz for the same transmission distance. If the transmitter antenna gain remains unchanged, a corresponding increase in receiver antenna gain is required to compensate for this additional attenuation. In practice, antenna arrays are often employed at mmWave frequencies to achieve higher directional gain, which will be discussed in later sections.

3.2 Shadowing, Scattering, and diffraction in non-LOS path transmissions.

When a direct LOS path is blocked, signals may still arrive at the receiver through mechanisms such as reflection, diffraction, and bending around obstacles. Due to their high operating frequencies and very short wavelengths, mmWave signals experience stronger shadowing and reflection effects, while diffraction plays a less significant role compared to lower-frequency systems. As a result, reflected components often dominate the received signal power.

Furthermore, the small wavelength of mmWave signals increases their sensitivity to environmental objects, causing greater signal fluctuations due to blockage, scattering, and reflection than in sub-6 GHz bands. The combination of enhanced diffuse scattering and weaker diffraction leads to more pronounced shadowing effects for mmWave propagation when compared with conventional lower-frequency wireless communications [1].

4 5G MOBILE PHONE ANTENNAS

Over the past ten to twenty years, the mobile phone has become an important tool for our daily life. The global market size was USD457 billion in 2021 and it was estimated the market will grow to 792 billion in 2029 with an average yearly growth rate of 7.3% [1]. Over one billion mobile phones are sold every year, and half of the world's population owns a smartphone. People typically use mobile phones to make phone calls, which use 4G modems and antennas. When people use WiFi at home or at work, WiFi antennas are used. Bluetooth antennas and GPS antennas are used when people listen to music or navigate on the highway. mmWave antennas are used when people watch 8K TV programmes from their smartphones. Always-on, high-speed connectivity is the basis for all these use scenarios and people expect their devices to be seamlessly connected; any connection problem can cause bad user experiences.

As of August 2024, only USA and Japan have active deployments of mmWave 5G networks. Most of the countries have deployed sub-6 GHz 5G only. Even for those countries that have deployed mmWave 5G networks, mmWave 5G is only available in downtown areas of certain cities due to the short range of mmWave coverage and expensive investments of mmWave towers and equipment. Smartphone manufacturers usually include mmWave hardware for selected regions where mmWave networks are available. For example, Apple iPhone12, iPhone13, iPhone14 support mmWave 5G networks in US. Outside of the United States and Japan, only sub-6 GHz 5G networks are supported. Below Table 2 shows Sub-6 GHz mid-band spectrum in different countries.

Table 2. Sub-6 GHz mid-band spectrum in different countries.

	Countries	1 to 3GHz Frequency band (GHz)	3 to 4GHz Frequency band (GHz)	4 to 5GHz Frequency band (GHz)
Asia	Korea	2.30-2.39	3.40-3.70 3.70-4.00	
	Japan		3.60-4.10	4.50-4.90
	China	2.50 or 2.60 (B41 or n41)	3.30-3.60	4.50-5.00
Europe	EU		3.40-3.80	
	France		3.46-3.80	
	Italy		3.60-3.80	
North America	USA	2.50-2.60	3.45-3.70 3.70-3.98	4.49
	Canada		3.47-3.65 6.65-4.00	

4.1 Sub-6 GHz Antennas and mmWave Antennas

Since mmWave signals are high-frequency signals, they can only cover a very short range. mmWave signals may face various issues, including multipath fading and atmospheric absorption losses. Due to these limitations and heavy investment of mmWave equipment, many countries have so far focused on investment of sub-6 GHz 5G, which offers great coverage with speeds faster than previous 4G networks.

mmWave represents electromagnetic waves that have extremely short wavelengths in the millimetre range. The shorter the wavelength, the higher the frequency. Because of the availability of wider bandwidths, higher-frequency signals can carry more data. Traditionally, the mmWave frequency band is used for radar detection in the aerospace industry as well as objection detection in the automotive industry.

4.2 Challenges in 5G Antenna Design

Although millimeter-wave technology enables extremely wide bandwidths, signals at these frequencies suffer from severe propagation impairments, including high free-space attenuation, molecular absorption in the atmosphere, poor penetration through common materials, and limited diffraction around physical obstructions [1]. To counteract these effects, mmWave communication systems must rely on antenna arrays capable of providing substantially higher directional gain.

4.2.1 Space limitations in future mobile phones to cater to additional bands and antennas.

Below Fig. 1 shows one example how mmWave antennas are placed inside of Samsung Galaxy S20 Ultra 5G smart phone. As we can see, the space inside the phone is very dense: most of the space is taken by the main board, battery, connectors and cameras. As a result, there is very little unused space. Three mmWave antennas are placed on two sides of the mobile phone, another mmWave antenna is put on the back side of the phone.

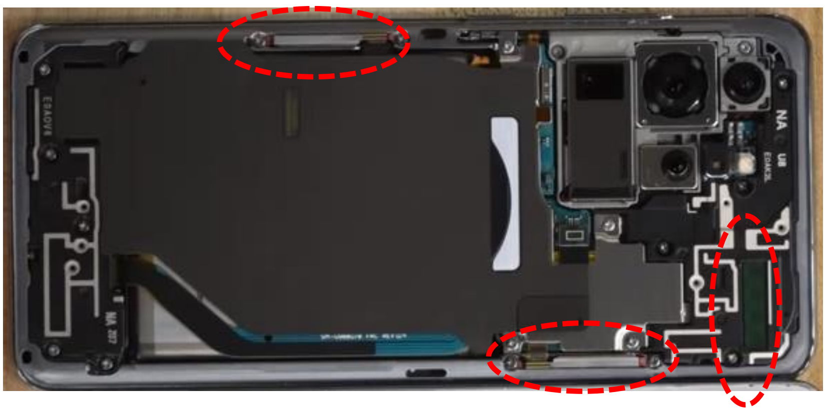

Fig. 1. Antennas inside 5G smart phone

It was estimated that operating frequency for future mobile wireless communication system will continue to increase, which will provide wider bandwidth. A wider bandwidth will increase the channel capacity according to Shannon theory. As a result, future mobile wireless communication system will require more antennas. On the other hand, mobile phone consumers are looking for slim and thinner phones for better user experience.

4.2.2 More sensitivity from the users on mobile phones on mmWave antennas

In everyday usage, mobile phones are held in a wide variety of orientations, such as portrait, landscape, or irregular positions. These variations, together with obstruction caused by the user's hand and head, can significantly degrade antenna performance. Previous studies, including early investigations on the Apple iPhone 4 in 2010, have demonstrated that antenna placement plays a critical role in determining user experience.

For 5G mobile terminals, antenna configurations must satisfy the minimum peak Equivalent Isotropic Radiated Power (EIRP) and spherical coverage requirements defined by 3GPP standards. According to 3GPP TS 38.521, user equipment (UE) is categorized into four power classes based on output capability, as summarized in Table 3 [3].

Compared with LTE systems, mmWave antennas experience substantially higher free-space path loss. To compensate for this increased attenuation, antenna arrays are typically employed to generate highly directional beams with enhanced gain [6]. However, narrow beams require accurate alignment with the base station. Since the orientation of a handheld device and the user's position cannot be predicted, mmWave antenna systems must support beam steering in order to maintain reliable connectivity under practical usage conditions [6].

4.3 Parameters to be considered when designing 5G mmWave antennas

4.3.1 Effective Isotropic Radiation Power (EIRP)

Effective Isotropic Radiated Power represents the power level that would be required from an ideal isotropic radiator to achieve the same maximum radiation intensity as the actual antenna. In practice, EIRP describes the radiated power measured in the direction of highest gain. It is related to the transmitter output power P_t, feeder losses L, and antenna gain G, and can be expressed as:

$$EIRP = P_t - L + G \tag{4}$$

If the directivity D of an antenna is known, we can get total radiated power (TRP) by below formula (5)

$$TRP = EIRP - D \tag{5}$$

Table 3. Minimum Peak EIRP requirement for UE with different power class [2]

UE Power Class	UE type
1	Fixed wireless access (FWA)UE
2	Vehicular UE
3	**Handheld UE**
4	High power non-handheld UE

Operating band	Power class 1 (Min Peak EIRP, dBm)	Power class 2 (Min Peak EIRP, dBm)	**Power class 3** (Min Peak EIRP, dBm)	Power class 4 (Min Peak EIRP, dBm)
n257	40.0	29	**22.4**	34
n258	40.0	29	**22.4**	34
n260	38.0	TBD	**20.6**	31
n261	40.0	29	**22.4**	34

4.3.2 50% percentile CDF

In the 3GPP specification, spherical coverage is specified by the cumulative distribution function (CDF) of EIRP, which is related to antenna gain and transmitted power. For 5G mobile phone design, designers need to simulate and check if the 50th percentile CDF meets the 3GPP specification requirement. 50th percentile CDF means that half of the sphere is covered with the required EIRP. Another parameter is the 100th percentile tile CDF which means the peak EIRP value of the antenna or antenna array. Table 4 shows the spherical coverage requirement for UE with different types of power classes.

Table 4. CDF requirements [2]

Operating band	Spherical Coverage (Unit: dBm)			
	85% tile CDF	60% tile CDF	**50% tile CDF**	20% tile CDF
n257	32.0	18.0	**11.5**	25
n258	32.0	18.0	**11.5**	25
n260	32.0	18.0	**8**	19
n261	32.0	18.0	**11.5**	25
UE Power Class	1	2	**3**	4

In conclusion, minimum Peak EIRP and 50th percentile CDF are important parameters when it comes to 5G antennas. 5G antennas should be designed in such way that they meet both coverage and gain requirements to get best possible antenna performance.

5 STATE OF THE ART 5G MOBILE PHONE ANTENNA SOLUTIONS

5.1 Eight-element phased arrays on two sides of mobile devices

Nowadays consumers prefer mobile phones with big touch screens and full metallic cases. Some researchers have proposed integrating the mmWave antennas into metallic case frames.

For example, Bin Yu et al. [3] have proposed to have one set of mmWave antenna arrays on each side of the mobile phone metal frames as shown in Fig. 2 below. In this configuration, the two longer edges of the metallic frame are primarily reserved for mmWave antenna arrays. The remaining sections are allocated to conventional sub-6 GHz 4G LTE and diversity MIMO antennas, as well as other wireless modules such as GPS and Wi-Fi antennas [3].

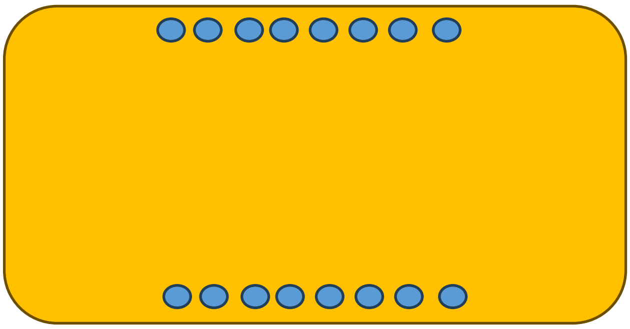

Fig. 2. Full view of mobile phone with mmWave antennas, redrawn from B. Yu, K. Yang et al. 2018 [3] .

Return loss

Fig. 3 presents both the simulated and measured reflection coefficient S_{11} and the isolation between adjacent antenna elements S_{21} . The measured resonant frequency, centered at approximately 28.5 GHz, shows a slight shift compared with the simulated result, which is likely attributable to fabrication tolerances. The measured −10 dB impedance bandwidth exceeds 2.5 GHz, covering roughly 27.5 GHz to 30 GHz, thereby fully satisfying the 5G spectrum requirements around the 28-GHz band (27.5–28.35 GHz). In addition, the measured mutual coupling between neighboring antenna ports remains below approximately −17 dB.

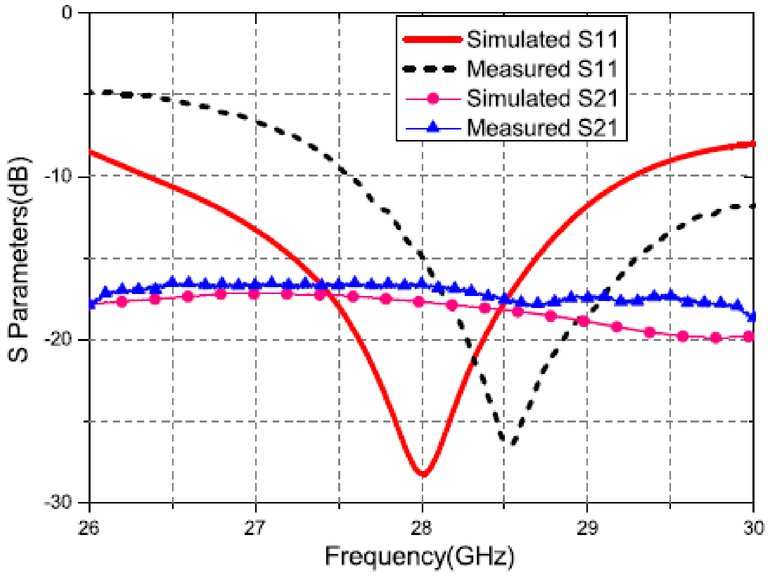

Fig. 3. Measured and simulated input reflection coefficients S11 and the isolation between two adjacent elements S21, reprinted, with permission, from B. Yu, K. Yang et al. 2018 [3] © 2018 IEEE.

Radiation pattern, Gain

Fig. 4 below shows the measured and simulated radiation patterns in E-plane and H-plane. The measured slot element gain was more than 6.5 dBi. [3]

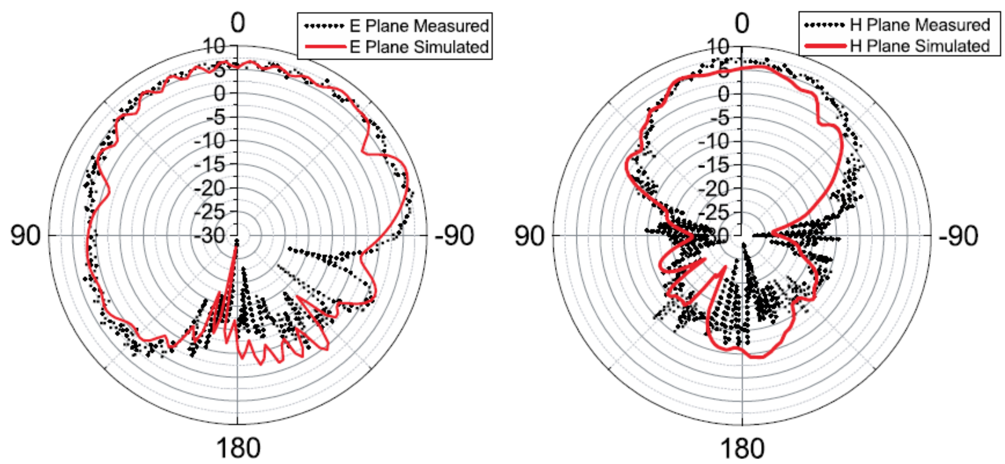

Fig. 4. Measured and simulated radiation patterns in E-plane and H-plane, reprinted with permission, from B. Yu, K. Yang et al. 2018 [3] © 2018 IEEE.

Beam Steering

The proposed antenna array demonstrates effective beam steering capability, enabling angular scanning over a range of approximately ±60°. Across the 0° to 30° steering range, the variation in realized gain remains within 1 dB, indicating stable radiation performance. When the steering angle increases from 30° to 60°, the gain decreases by only a few decibels. The peak gain is approximately 15.6 dBi at boresight (0°), while the minimum recorded gain is around 12 dBi at a steering angle of 60°.

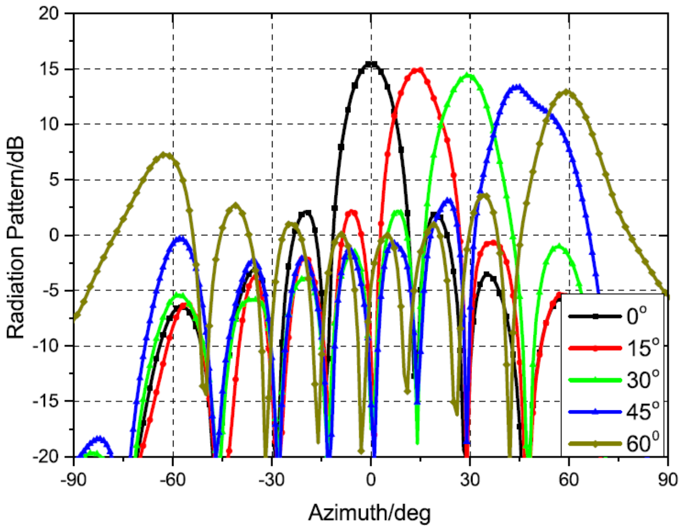

Fig. 5. Beam steering radiation pattern, reprinted with permission, from B. Yu, K. Yang et al. 2018 [3] © 2018 IEEE.

User's effects on antenna performance

When the user's thumb partially covers the left edge of the device, the eight-element phased array located on that side experiences a relatively modest gain reduction of approximately 5.4 dB. In contrast, the antenna array positioned on the right edge undergoes more significant degradation, with a measured gain decrease of up to about 8.7 dB. This difference is primarily attributed to the greater extent of coverage by the user's fingers along the right-hand side of the handset.

5.2 Co-Designed mmWave and LTE Antennas

Researchers from Aalto University, Joni Kurvinen *et al.* proposed both mmWave and LTE antennas that can be accommodated in a shared volume. The proposed design in the paper [7] supports LTE LB and HB at 700-960 MHz and 1710-2690 MHz, respectively, besides the mmWave band at 25-30 GHz. [7] The design was divided into three steps. First, the mmWave antenna was simulated and designed separately without considering the LTE antennas. Secondly, the LTE antennas were designed, but the mmWave antenna was taken into consideration when designing the LTE antennas. The final step is the co-design by embedding the mmWave module to the LTE antenna, and some fine-tuning of the dimensions and redesigning of the matching circuit was done to achieve the desired performance [7].

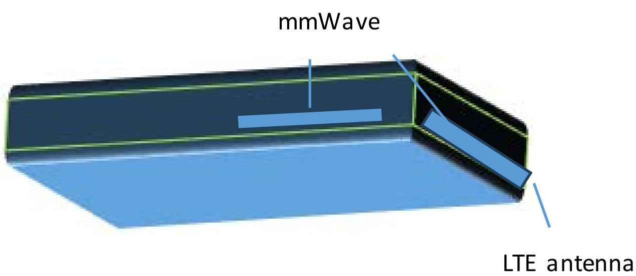

Fig. 6. mmWave modules together with LTE main antenna, redrawn from [7].

5.2.1 Performance Objectives

The performance of the combined antenna system is assessed based on impedance matching, total radiation efficiency, and beam-steering capability for the mmWave module. For the LTE antennas, the design goals include a reflection coefficient better than −6 dB and a total efficiency of at least 60%. Furthermore, isolation between the low-band and high-band LTE antennas is required to exceed 15 dB.

For the mmWave antenna, the impedance matching target is set below −10 dB, while a realized gain above 6 dBi is desired, together with the capability to electronically steer the main beam over a minimum angular range of ±25°.

5.2.2 Antenna Structures

The mobile handset is modelled, and the antenna configurations are developed and analysed using the full-wave electromagnetic simulation software CST Microwave Studio [7]. To efficiently utilize the limited internal space, the LTE antennas are positioned along the side rim of the device. The mmWave antenna is implemented on a dedicated printed circuit board using a 0.101-mm-thick Rogers RO4350B substrate ($\varepsilon r = 3.48$, $\tan\delta = 0.0037$) and encapsulated in a plastic enclosure fabricated from PREPERM L450 material ($\varepsilon r = 4.5$, $\tan\delta = 0.0005$) for RF optimization. The finalized co-designed LTE and mmWave antenna structure is illustrated in Figure 8.

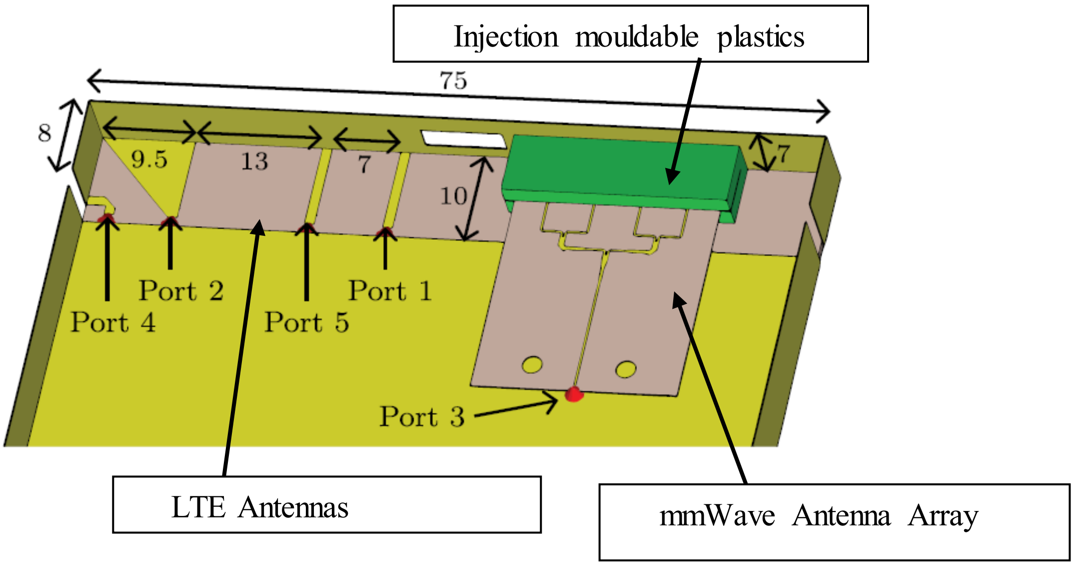

Fig. 7. Structure of co-designed antennas, reprinted, with permission, from J. Kurvinen et al. [7] © 2019 IEEE.

The mmWave antenna array is enclosed inside a plastic, which is used to cover the aperture that allows the antenna to radiate through the metal rim, as shown in below 7.

Fig. 8. Plastic-filled window in the metal rim for the mmWave antennas, adapted, with permission, from [7] © 2019 IEEE.

The prototype was manufactured based on the simulation model and specifications by the team as shown in Fig. 9 below.

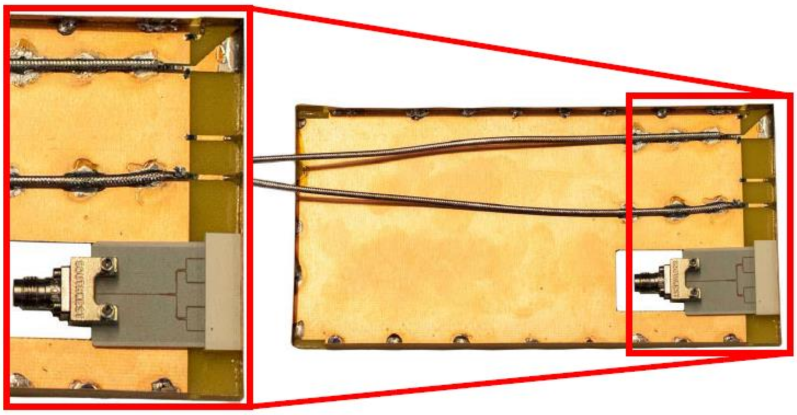

Fig. 9. Manufactured prototype, reprinted, with permission, from J. Kurvinen et al. [7] © 2019 IEEE.

5.2.3 mm-Wave performance

The input matching characteristics of the antenna system were evaluated for three beam steering configurations corresponding to phase shift settings that produce steering angles of approximately 0°, 50°, and 100°. Both simulated and measured results were obtained using prototype implementations. Across the operating frequency range, the reflection coefficient remains below −10 dB for all three configurations, indicating stable impedance behaviour despite minor discrepancies between simulated and measured responses.

To realize the required progressive phase shifts, three distinct printed circuit board (PCB) implementations were employed, each providing a different phase response within the antenna array. This approach enables beam steering while maintaining consistent impedance performance across the considered configurations.

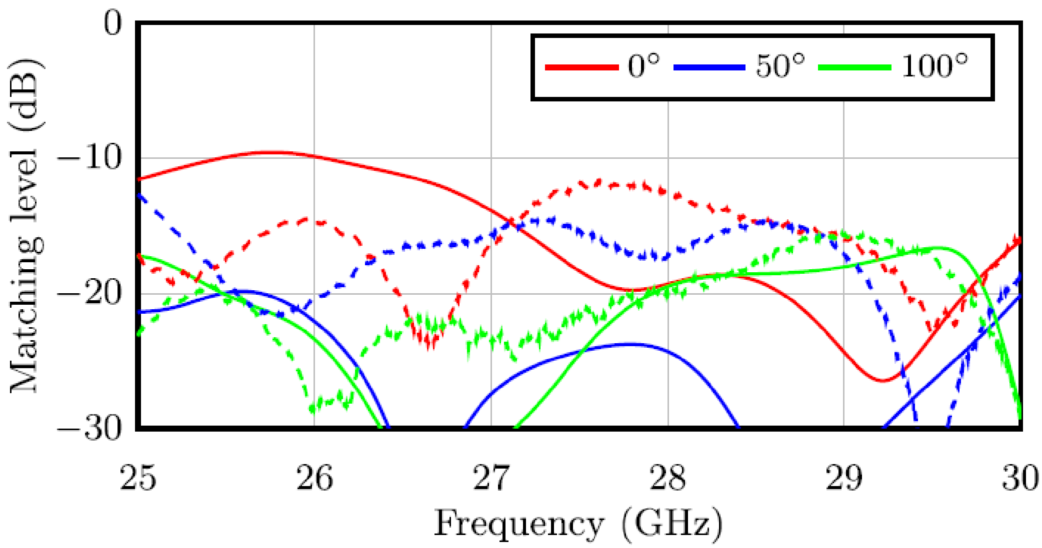

Fig. 10. Measured and simulated input matching for three implemented phase shifter configurations corresponding to steering angles of 0°, 50°, and 100°. Reproduced, with permission, from J. Kurvinen et al. [7], © 2019 IEEE.

Fig. 11 illustrates the radiation characteristics of the antenna array at 26 GHz. The measured patterns demonstrate effective beam steering behaviour, with the main radiation lobe shifting within an angular range of approximately ±30°. The corresponding peak realized gain is observed to fall within the range of 5–7 dBi, depending on the selected phase shift configuration.

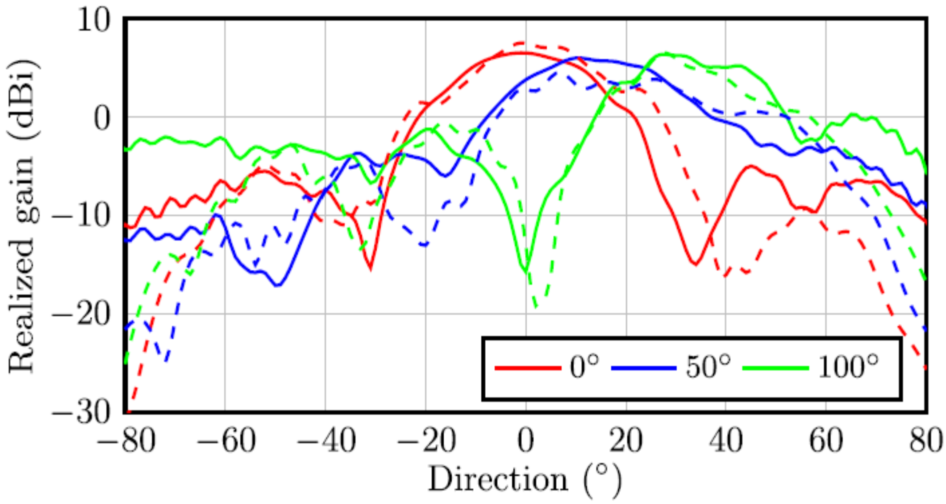

Fig. 11. Realized gain patterns of the antenna array at 26 GHz, reprinted, with permission, from J. Kurvinen et al. [7] © 2019 IEEE.

Fig. 12 below shows the beam steering capability at 28 GHz, and the measured peak values are around 2 dB less than the simulated values. Inaccuracies in the manufacturing process might cause this. The desired beam steering directions are also achieved, with the maximum at around ±40°.

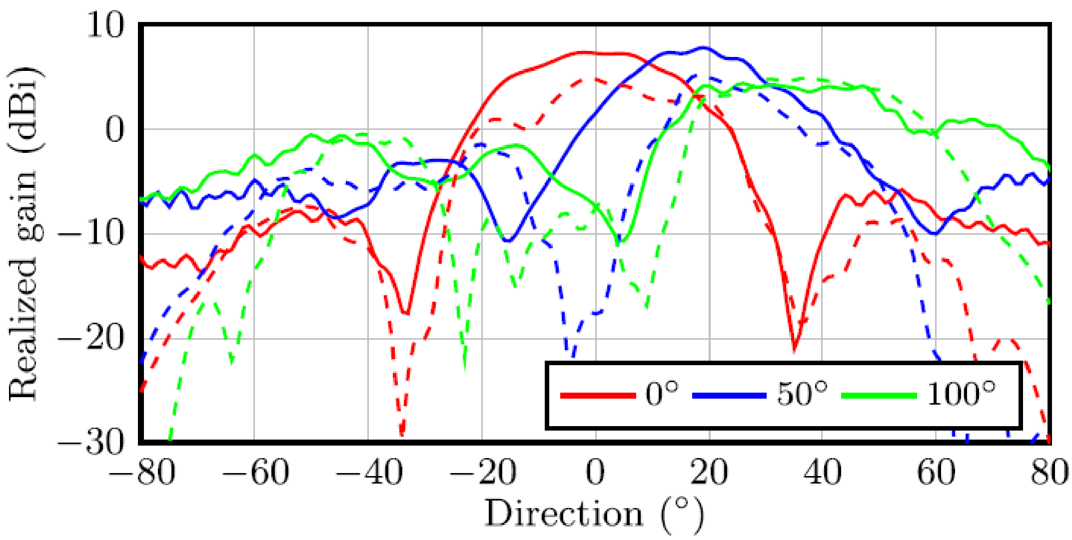

Fig. 12. Realized gain patterns of antenna array at 28 GHz, reprinted, with permission, from J. Kurvinen et al. [7] © 2019 IEEE.

5.3 mmWave antenna arrays in two corners of mobile phones

Wonbin Hong *et al.* [8] proposed to have two mmWave antenna arrays assembled at the top right corner and bottom left corners of mobile phones as illustrated in below picture (B) of Fig 13. Fig. 13 (A) shows one Samsung smartphone with LTE, GPS, WIFI, Bluetooth antennas.

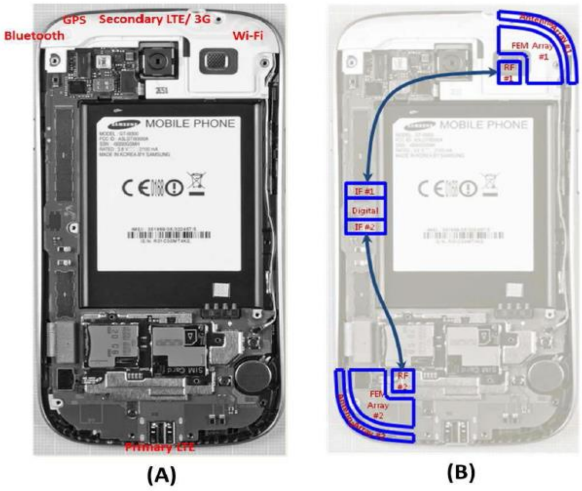

Fig. 13. (A) Antenna placement in 4G Samsung smartphone (B) Proposed mmWave antenna lay-out, reprinted, with permission, from W. Hong et al. [8] © 2017 IEEE.

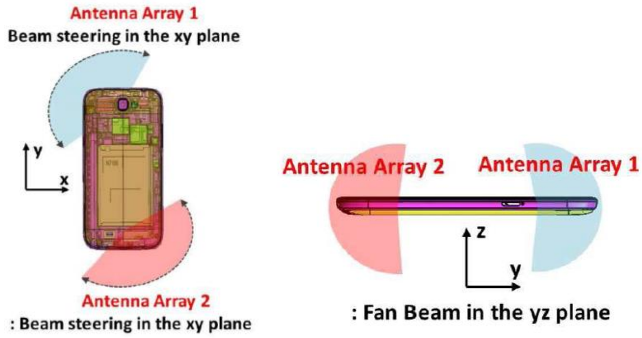

Fig. 14. Proposed mmWave 5G antenna placement, reprinted, with permission, from W. Hong et al. [8] © 2017 IEEE.

In this paper, detailed simulations were not performed for such antenna design, so we are not able to compare the performance differences between this and other solutions.

5.4 Antenna On Display (AoD) and Antenna in Display (AiD)

Advanced antenna integration technologies, including Antenna-on-Chip (AoC), Antenna-on-Package (AoP), and Antenna-in-Package (AiP), have been widely adopted as practical solutions for millimeter-wave (mmWave) implementation in 5G mobile devices. These approaches enable compact integration of antenna elements with radio-frequency circuitry, which is essential for accommodating mmWave functionality within the limited form factor of modern smartphones. Representative commercial implementations demonstrate that multiple mmWave antenna modules are typically distributed around the device to enhance spatial diversity and mitigate the severe propagation challenges associated with mmWave frequencies [9].

In recent years, increasing attention has been directed toward integrating antenna elements with the display structure of smartphones, leading to the development of Antenna-on-Display (AoD) and Antenna-in-Display (AiD) concepts. These approaches aim to exploit the available surface area of the display region while maintaining acceptable optical transparency and user experience. Various design strategies have been explored to balance electromagnetic performance with optical and manufacturing constraints, including the use of transparent conductive materials and non-optical display regions for antenna placement [10], [11].

AoD-based solutions generally place antenna elements on top of the display layer, which can simplify antenna integration but may introduce trade-offs between radiation efficiency and optical transparency. In contrast, AiD approaches embed antenna structures within or beneath the display stack, allowing improved integration with the device chassis and enhanced conductive pathways. This configuration can offer advantages in terms of impedance stability and overall antenna performance, although it may impose additional constraints on display manufacturing processes and mechanical design [10].

Overall, both AoD and AiD techniques represent promising directions for mmWave antenna integration in future smartphone platforms. Their relative performance depends strongly on material selection, antenna placement, and system-level co-design considerations, highlighting the importance of jointly optimizing electromagnetic, optical, and mechanical requirements.

5.5 Performance Summary of Different Solutions

Table 5 summarizes the reported performance characteristics of representative mmWave antenna integration solutions for 5G mobile devices. The comparison highlights the trade-offs among antenna gain, beam steering capability, and integration complexity associated with different design approaches. Solution of applying two antenna arrays on two sides of mobile phones achieved good beam steering capability and good gain at 6.5dBi. Solutions employing optically transparent antenna structures can achieve best radiation performance, with Gain at 13.32 dBi. Whereas designs utilizing non-optical regions of the device often demonstrate improved beam steering capability and higher realized gain [10], [11]. These results indicate that no single integration strategy universally outperforms others across all performance metrics. Instead, the selection of an appropriate antenna solution depends on the specific design objectives and constraints of the target application, including display requirements, device form factor, and beam steering performance.

Table 5. Performance comparison of different solutions.

Reference	Reflection coefficients S11	Mutual coupling S21	Gain	Beam steering
[3]	10 dB return loss bandwidth ≥2.5GHz	S21≤-17 dB	≥6.5 dBi	±60°
[7]	1710-2690 MHz	Not verified	5-7 dBi	±25°
[8]	60 GHz	Not verified	Not verified	Not verified
[11]	25.6-31.9 GHz	Not verified	12.32 dBi	No verified
[12]	Centre frequency 28 GHz	Not verified	9.16 dBi	±60°

6 MMWAVE ANTENNA USER EFFECT AND SAR STANDARDS

6.1 Concept of Specific Absorption Rate

In radio-frequency exposure evaluation, specific absorption rate (SAR) is used as a quantitative metric to describe how electromagnetic energy is absorbed by biological tissue. SAR represents the rate at which RF power is deposited per unit mass of tissue and is determined by the interaction between the incident electromagnetic field and the electrical properties of the medium.

From an electromagnetic perspective, SAR depends on the local electric field intensity, tissue conductivity, and mass density. Therefore, SAR provides a practical means to assess potential thermal effects caused by RF exposure in wireless communication systems. The general mathematical relationship of SAR can be expressed as

$$\mathrm{SAR}=\frac{d}{dt}\left(\frac{dw}{dm}\right)=\frac{d}{dt}\left(\frac{dW}{\rho dv}\right) \tag{6}$$

6.2 SAR Standards

To ensure user safety, regulatory bodies worldwide have established limits for human exposure to radio-frequency electromagnetic fields. These regulations are based on extensive biological and electromagnetic studies and aim to prevent excessive tissue heating during device operation.

In practical wireless system evaluation, exposure limits differ according to frequency range and measurement methodology. At lower microwave frequencies, electromagnetic fields can penetrate deeper into biological tissue, making localized energy absorption a primary concern. In this regime, SAR-based limits are commonly applied.

As operating frequency increases toward the millimetre-wave range, electromagnetic energy becomes increasingly confined to superficial tissue layers. Consequently, incident power density rather than volumetric energy absorption becomes a more appropriate metric for exposure assessment. For this reason, international guidelines transition from SAR-based evaluation to power-density-based limits at higher frequencies.

Below are four major SAR standards, recognized globally in the wireless communication industry, covering US, Europe, and Asia.

6.2.1 FCC 47 CFR 1.1310

The FCC has set SAR limits for frequencies between 100 kHz and 6 GHz, as shown in Table 6 below. Limits are set for both general population conditions and occupational conditions.

Table 6. SAR limits for frequency range 100 kHz to 6 GHz, adapted from [9].

Conditions	Whole Body Exposure (W/kg)	Peak spatial-average SAR (W/kg)	Local Exposure (W/kg)	Max Exposure (Minutes)
SAR limit for the General Population	0,08	1,6	4	6

SAR limit for Occupational Person	0,4	8	20	30

6.2.2 IEEE Standard: C95.1-2019

The IEEE C95.1-2019 standard defines dosimetric reference limits (DRLs) to regulate human exposure to radio-frequency electromagnetic fields across a wide frequency range. For operating frequencies below 6 GHz, exposure compliance is primarily evaluated using specific absorption rate (SAR), which quantifies the absorbed RF energy within biological tissue.

Different SAR limits are specified depending on exposure conditions. More conservative thresholds are applied to the general public, while higher limits are permitted for occupational exposure, reflecting differences in controlled environments and user awareness. SAR constraints are further categorized into whole-body averaged exposure and localized exposure for specific body regions, such as the head, torso, and limbs.

When the operating frequency exceeds 6 GHz and extends into the millimetre-wave band, the IEEE standard transitions from SAR-based evaluation to epithelial power density metrics. In this frequency range, RF energy is predominantly absorbed at the skin surface, making surface-averaged power density a more representative measure of user exposure. The evaluation involves spatial averaging over a defined surface area and temporal averaging to account for variations in transmitted power.

6.2.3 ICNIRP Standard

The International Commission on Non-Ionizing Radiation Protection (ICNIRP) has established internationally recognized guidelines for limiting human exposure to time-varying electromagnetic fields. Initially released in the late 1990s and updated in 2020, these guidelines cover frequencies up to 300 GHz and are widely adopted across regulatory frameworks.

For frequencies below 6 GHz, ICNIRP specifies SAR-based basic restrictions similar in concept to those defined by IEEE standards. These include limits on whole-body averaged SAR as well as localized SAR for specific anatomical regions. Separate limits are defined for the general population and occupational exposure scenarios to ensure appropriate safety margins.

At frequencies above 6 GHz, ICNIRP replaces localized SAR limits with surface-averaged incident power density constraints, reflecting the reduced penetration depth of millimetre-wave signals. In this regime, exposure assessment focuses on spatial peak power density averaged over a standardized surface area, ensuring protection against excessive superficial heating effects.

6.2.4 Australia Radiation Protection Standard: ARPANSA RPS3 2002

In Australia, radio-frequency exposure limits are regulated under the ARPANSA RPS3 standard, which defines maximum permissible exposure levels for frequencies ranging from kilohertz to millimeter-wave bands. This standard incorporates both SAR-based and power-density-based evaluation methods, depending on the operating frequency.

For frequencies below 6 GHz, ARPANSA specifies SAR limits for whole-body and localized exposure, consistent with international safety principles. In addition, spatial peak specific absorption limits are applied to restrict localized energy concentration within small tissue volumes.

At higher frequencies, particularly in the millimeter-wave region, ARPANSA adopts surface-based exposure metrics to control peak spatial power density. These limits are designed to prevent rapid superficial heating effects, which are the dominant interaction mechanism at such frequencies.

6.3 Implications for mmWave Antenn Design

The shift from SAR-based evaluation to power-density-based assessment has direct implications for mmWave antenna design. Antenna placement, beam steering range, and near-field characteristics must be carefully optimized to ensure compliance under worst-case operating conditions.

Therefore, understanding SAR principles and regulatory exposure metrics remains essential for the safe and compliant design of mmWave antenna systems, especially in user-proximity scenarios such as handheld and wearable devices.

7 DESIGNING MILLIMETER WAVE ANTENNAS FOR MOBILE PHONE

As discussed in previous chapters, two of the most significant challenges in mmWave mobile phone antenna design are space limitations and sensitivity to user interactions. To address these challenges, several key design principles must be considered.

Antenna Size Reduction
To meet the beam-steering requirements of mmWave antennas, multiple mmWave antenna modules may need to be integrated within a single mobile phone. Therefore, designing compact and efficient antennas is essential to accommodate them within the limited space. One effective approach is the use of antenna arrays, which allow for improved gain and beamforming capabilities while maintaining a compact footprint. Additionally, integrating mmWave antennas within the mobile phone's display, chassis, or frame can further optimize space utilization without compromising performance. Advanced fabrication techniques, such as transparent antennas or embedded antenna structures, can be explored to enhance integration while maintaining the aesthetic and functional aspects of the device.

Minimizing Sensitivity to User Interaction
User movement and changes in phone orientation can significantly affect mmWave antenna performance due to the directional nature of mmWave signals. To mitigate this, mmWave antennas must support beamforming and beam-steering techniques, which dynamically adjust the antenna's radiation pattern in real-time to maintain a strong connection. Furthermore, since 5G mobile phones are equipped with multiple mmWave antennas, Multiple Input Multiple Output (MIMO) technology is essential. MIMO enables multiple antennas to simultaneously transmit and receive signals, improving signal robustness, throughput, and overall network reliability.

Compliance with Regulatory and Performance Standards
mmWave antennas must adhere to strict performance and safety regulations. One key requirement is achieving the specified Effective Isotropic Radiated Power (EIRP) and spherical coverage, as defined by 3GPP specifications. Additionally, antennas must comply with global Specific Absorption Rate (SAR) standards, ensuring user safety by limiting electromagnetic exposure. Regulatory bodies such as the FCC (47 CFR 1.1310) and standards organizations like IEEE (C95.1-2019) establish guidelines for permissible exposure levels and radiation limits. Compliance with these standards is crucial to obtaining certification and ensuring the commercial viability of mmWave-enabled mobile devices.

8 CONCLUSIONS AND FUTURE WORK

This bachelor's thesis highlighted design challenges for 5G mobile phone mmWave antenna designs. 5G mobile phones need to support more frequency bands, which means that more antennas are needed for 5G mobile phones. On the other hand, 5G mobile phones are getting thinner, which leaves less space for antennas. After reviewing some of the state-of-the-art mmWave antenna designs, it was found out that antenna arrays on both side of mobile phone , optically transparent antenna structures and antennas in display using non optical space can achieve good radiation and beam steering performance.

Antenna arrays can offer several benefits over single antenna designs because antenna arrays can offer increased gain compared to a single antenna. An antenna array can also be used for beamforming, which transfer the signals to specific directions. Antenna arrays can help mitigate interference by steering the beams in a specific direction that will reduce the impact of interference from other sources. An antenna array can also provide diversity in communication that can improve reliability and reduce the impact of interference. Diversity can be achieved by transmitting the same signals from multiple antennas or transmitting different signals from each of the antennas.

Antenna on non-optical region can achieve gain at 12.32dBi, and with good beam steering capability, antennas in display using non optical space can achieve gain at 9.16 dBi, with beam steering at ±60°.

Major SAR standards and SAR limits for Sub-6 GHz and mmWave frequencies were summarized and compared in the second part of the thesis. These SAR standards and limits should be followed when making 5G mmWave antenna design.

Finally, it summarizes design principles of mmWave antennas for mobile phones. It highlights compact antenna integration using array-based architectures and advanced packaging techniques, as well as adaptive beamforming, beam-steering, and MIMO technologies to maintain link reliability under dynamic usage conditions. It also emphasizes the importance of compliance with regulatory and safety standards, including EIRP, spherical coverage, and SAR requirements, which are essential for certification and commercial deployment of mmWave-enabled mobile devices.

I would like to simulate and evaluate antenna arrays to 5G phones in more detail as my future work, it might be a good idea to make a 5G mmWave antenna prototype and compare the measurement results with the simulation data.

9 REFERENCES

[1] R. Ludwig, "Who cares about latency in 5G?" *Ericsson Blog*, Aug. 2022. [Online]. Available: https://www.ericsson.com/en/blog/2022/8/who-cares-about-latency-in-5g.

[2] 3GPP, "NR; user equipment (UE) radio transmission and reception; Part 2: Range 2 standalone," *3GPP TS 38.101-2*, V15.23.0, Release 15, Dec. 2022. [Online]. Available: https://www.3gpp.org

[3] B. Yu, K. Yang, C.-Y.-D. Sim, and G. Yang, "A novel 28 GHz beam-steering array for 5G mobile device with metallic casing application," *IEEE Transactions on Antennas and Propagation*, vol. 66, no. 1, pp. 462–466, Jan. 2018, doi: 10.1109/TAP.2017.2772084.

[4] D. M. Pozar, "Microstrip antennas," *Proceedings of the IEEE*, vol. 80, no. 1, pp. 79–91, Jan. 1992, doi: 10.1109/5.119568.

[5] W. Roh *et al.*, "Millimeter-wave beamforming as an enabling technology for 5G cellular communications: Theoretical feasibility and prototype results," *IEEE Communications Magazine*, vol. 52, no. 2, pp. 106–113, Feb. 2014, doi: 10.1109/MCOM.2014.6736750.

[6] T. S. Rappaport, R. W. Heath, R. C. Daniels, and J. N. Murdock, *Millimeter Wave Wireless Communications*, 1st ed., Upper Saddle River, NJ: Prentice Hall, 2014.

[7] J. Kurvinen, H. Kähkönen, A. Lehtovuori, J. Ala-Laurinaho, and V. Viikari, "Co-designed mm-wave and LTE handset antennas," *IEEE Transactions on Antennas and Propagation*, vol. 67, no. 3, pp. 1545–1553, Mar. 2019.

[8] W. Hong, K.-H. Baek, and S. Ko, "Millimeter-wave 5G antennas for smartphones: Overview and experimental demonstration," *IEEE Transactions on Antennas and Propagation*, vol. 65, no. 12, pp. 6250–6261, Dec. 2017, doi: 10.1109/TAP.2017.2740963.

[9] Code of Federal Regulations, title 47, part 1.1310. FCC, 2016

[10] W. Lam, "Apple shows new levels of RF design complexity," *CCS Insight*, 2020. [Online]. Available: https://www.ccsinsight.com/blog/apple-shows-new-levels-of-rf-design-complexity/

[11] J. Park, S. Y. Lee, J. Kim, D. Park, W. Choi, and W. Hong, "An optically invisible antenna-on-display concept for millimeter-wave 5G cellular devices," *IEEE Transactions on Antennas and Propagation*, vol. 67, no. 5, pp. 2942–2951, May 2019.

[12] J. Oh, B. Kim, S. Yoon, K. Kim, E. J. Sung, and J. Oh, "High-gain millimeter-wave antenna-in-display using non-optical space for 5G smartphones," *IEEE Transactions on Antennas and Propagation*, vol. 71, no. 2, pp. 1458–1466, Feb. 2023.

[13] IEEE Standard for Safety Levels with Respect to Human Exposure to Radio Frequency Electromagnetic Fields, 3 kHz to 300 GHz, IEEE Std C95.1-2006, 2006.

[14] IEEE Standard for Safety Levels with Respect to Human Exposure to Electric, Magnetic, and Electromagnetic Fields, 0 Hz to 300 GHz, IEEE Std C95.1-2019, 2019.

[15] ICNIRP, "Guidelines for limiting exposure to electromagnetic fields (100 kHz to 300 GHz)," *Health Physics*, vol. 118, no. 00, pp. 000–000, 2020, pre-print. doi: 10.1097/HP.0000000000001210.

[16] Australian Radiation Protection and Nuclear Safety Agency (ARPANSA), *Radiation Protection Standard for Maximum Exposure Levels to Radiofrequency Fields - 3 kHz to 300 GHz*, 2002.